# Structural variants contribute to the gut microbiome, blood metabolic traits and their causal relationships

Qun Zhou[1,†], Keqing Wang[2,†], Junhong Chen[1,†], Xinjiang Tan[2], Xin Jin[2], Shaoqiao Zhang[1], Liang Xiao[2,4], Tao Zhang[1,5*], Xiaomin Liu[1,5*]

1. BGI Research, Wuhan 430074, China;
2. BGI Research, Shenzhen 518083, China;
3. James D. Watson Institute of Genome Sciences, Hangzhou 310058, China;
4. Shenzhen Engineering Laboratory of Detection and Intervention of Human Intestinal Microbiome, BGI-Shenzhen, Shenzhen 518083, China;
5. Shenzhen Key Laboratory of Human Commensal Microorganisms and Health Research, BGI Research, Shenzhen 518083, China

[†] These authors contributed equally.
* To whom correspondence should be addressed: X.L., liuxiaomin@genomics.cn and T.Z., tao.zhang@genomics.cn

## Highlights

- Provides a catalog of 138,859 high-confidence SVs and 49.57% of which were novel based on 42× WGS of 2,002 individuals
- Identify 30 genome-wide significant "SVs—microbial taxa/pathways" and 48 "SVs—blood metabolites" associations, respectively
- An Asian-specific 6.5k deletion at *TENT2* gene strongly associated with the species *Coprobacillus sp. 29_1*
- A deletion spanning *HBA1/HBA2/HBM/HBQ118* associated with 9 blood metabolic traits, with most significant for the mean corpuscular volume (MCV)
- The majority of SVs demonstrated a more pronounced impact than neighboring SNPs in the associations with microbiome/metabolites
- SVs help to reveal the host-microbe interactions

**Abstract**

Genetic variants influencing the gut microbiome and blood metabolites have predominantly centered on the single nucleotide variants (SNPs), leaving the impact of structural variants (SVs) largely unexplored. Here, we applied an advanced structural variant calling pipeline to whole-genome sequencing data from 2,002 individuals with a mean depth of 42 folds, revealing 138,859 high-confidence SVs, of which 49.57% were not previously reported. Genome-wide association analyses were conducted for 22,519 common SVs with 616 gut microbial features and 121 blood metabolic traits, uncovering 30 significant associations between SVs and microbial taxa/pathways, as well as 48 associations between SVs and blood metabolites. Noteworthy findings include 19 associations meeting study-wide significance, such as the Asian-specific 6.5k deletion at *TENT2* gene strongly linked to species *Coprobacillus sp. 29_1* ($\beta$= 0.158, $p$ =2.5 × $10^{-9}$) and a deletion spanning *HBA1/HBA2/HBM/HBQ118* associated with 9 blood metabolic traits (most significant for the mean corpuscular volume (MCV), $\beta$= -0.570, $p$ = $1.22\times10^{-91}$). The majority of SVs demonstrated a more pronounced impact than neighboring SNPs in their associations with microbiome/metabolites. Furthermore, Mendelian randomization using SVs reveal the causal relationships between microbiome and metabolites, such as the causal effect of *Clostridium ramosum* on serum uric acid and MCHC on MF0064: the triacylglycerol degradation. This study presents a comprehensive SV catalog in the Chinese population and emphasizes the substantial contribution of SVs to the gut microbiome, blood metabolites and their interactions.

**Keywords**: structural variants, genome-wide association analysis, gut microbiome, blood metabolites, host-microbe interaction

## Introduction

The human gut microbiome plays a pivotal role in numerous physiological processes and is closely linked to our health as well as the development of diseases such as obesity[1,2], diabetes[3,4], inflammatory bowel disease[5,6], rheumatoid arthritis[7,8], cardiovascular diseases[9], and mental disorders[10,11]. Apart from being influenced by factors like environment, diet, lifestyle, and diseases, the gut microbiome is also controlled to some extent by host genetic factors[12,13]. In recent years, a number of microbial genome-wide association studies (mbGWAS) have identified various host genetic variants, including the frequently discussed *LCT* and *ABO* loci, that influence the gut microbiome[14-18]. However, except for the human microbiome project (HMP) and our prior research[19,20], nearly all mbGWAS studies have utilized genotyping arrays to investigate the impact of human single nucleotide polymorphisms (SNPs) on the microbiome, neglecting the potential impact of more extensive and intricate genomic variations.

Structural variations (SVs) constitute a significant form of genomic variation, including alterations exceeding 50 base pairs (bp) in length such as deletion (DEL), insertion (INS), inversion (INV), duplication (DUP), and copy number variants (CNVs). These SVs are prevalent in the human genome and have been associated with various disease phenotypes[21-24]. A recent study identified a correlation between CNVs of the human salivary amylase gene (*AMY1*) and the relative abundance of the genus *Ruminococcus* in the gut microbiome[25]. However, this study solely relied on PCR technology to explore the impact of a single human *AMY1* gene copy number variation on the microbiome. Given that few studies had both whole genome and whole metagenome data in the same cohort, thus to date, the impact of host SVs on the gut microbiome remains largely unexplored.

Not only the gut microbiome, the genome-wide contributions of host SVs to blood metabolic traits have been underexplored. Very limited evidences were reported. For example, Chen et al. identified a deletion of the *ALB* promoter and a CNV at *PDPR* that were significantly associated with blood metabolic traits in the Finish population[26]. The NHLBI TOPMed program has reported 21 independent SVs or 41 SV-trait associations across the total 24 quantitative hematologic traits[27]. These studies have been performed on mainly the European population. A recent study using the long-read sequencing

identified 22 SVs on 14 chromosomes associated with 13 phenotypes in the Chinese population[28]. However, the association analysis was conducted on no more than 327 individuals. Therefore, a detailed investigation into the extent to which SVs contribute to blood metabolic traits in the Asian population with a larger sample size is necessary. Moreover, comprehensively and systematically excavating the impact of host SVs on both the microbiome and metabolites using high-depth whole-genome data from a well-designed cohort will enhance our understanding of the host-microbiome interaction mechanisms.

In this study, we constructed and characterized a high-quality SV profile of the Chinese population based on 2,002 individuals from the 4D-SZ cohort[14,19,20,29-31], a multi-omics cohort comprising high-depth whole genome and metagenomics sequencing, blood metabolites, and detailed questionnaires. Subsequently, we conducted genome-wide association analyses to identify SVs that significantly contributed to the gut microbial taxa/pathways and blood metabolic traits, respectively. Moreover, we examined the intricate relationship between gut microbiome and blood metabolites through their associated SVs as mediators (see **Graphic abstract**). The primary objective of this study is to characterize the landscape of SVs in the Chinese population and unearth novel SVs associated with the microbiome and metabolites while offering valuable insights into the mechanisms governing host-microbiome interactions.

## Results

### Characterization of SVs identified in the Chinese population

We utilized high-depth whole-genome sequencing (WGS) data to identify SVs for 2,002 Chinese individuals from the 4D-SZ cohort. Among the sequenced samples, 53% were females, with an average age of 30 years ranging from 21 to 67 years (**Supplementary Fig. 1**). The mean sequencing depth per individual was 42×, amounting to an average of 122.46 Gb sequenced (**Supplementary Fig. 2a**). The base mapping rate varied from 96.74% to 100%, with an average of up to 99.89% (**Supplementary Fig. 2b).** An advanced Genome Analysis Toolkit's Structural Variant (GATK-SV) pipeline[32,33] was employed to detect SVs (**Supplementary Fig. 3**; Methods). Following rigorous quality control measures for both samples and variants, a total of 1,839 samples were retained. We detected a total of 138,859 high-confidence

SVs with quality scores surpassing 250 or marked as "PASS," while excluding "BND" variant types (**Supplementary Table 1)**. These SVs comprised 73,288 insertions (INSs), 38,782 deletions (DELs), 25,030 duplications (DUPs), 1,153 complex SVs (CPXs), 378 inversions (INVs), and 228 copy number variations (CNVs) (**Fig. 1a**). The most prevalent SV types were INSs, accounting for 52.78% of all SVs, followed by DELs representing 27.93% (**Fig. 1a**).

Despite the overall higher count of INSs compared to DELs in the population, each individual exhibited a greater number of DELs than INSs, consistent with an early study[34]. On average, each genome harbored 11,493 SVs events (ranging from 7,851 to 21,324), exceeding the SV count documented in the 1000genome phase3 (9,679 SVs; average depth of 30×) and the Genome Aggregation Database (gnomAD[32]; 7,439 SVs; average depth of 32×), yet lower than a long-read sequencing study[28] (18,489 SVs; average depth of 17×). DELs and INSs continued to be the most prevalent SV types, constituting 41.5% and 35.5% of all identified SVs, respectively. The average number of DELs, INSs, DUPs, CNVs, CPXs, and INVs per sample was 4,769, 4,075, 2,177, 237, 174, and 62, respectively (**Fig. 1b**).

For evaluating the identified SVs, we also applied the same sequencing and analysis methods on the cell line from the reference sample NA12878 (**Methods**). Through the application of the GATK-SV pipeline, 10,624 SVs were detected. Comparison of the detected SVs to the gold standard truth set of NA12878[35] revealed precisions of 79.5% for deletions, 64.2% for duplications, 69.4% for insertions, and 75% for inversions. Additionally, the impact of sequencing depth on SV detection was assessed, as shown in **Supplementary Fig. 4**. Overall, a higher sequencing depth was correlated with an increased number of SVs, with a gradual rise in SV counts from 20× to 50×**.** However, this trend declined beyond 50×, potentially due to the limited number of samples.

Across all population-detected SVs, 71.55% were rare with minor allele frequencies (MAF) below 1%. Most SVs exhibited lengths distributed within the range of 50~100bp (61.02%) and 100-500bp (15.77%; **Fig. 1c**). Expected peaks corresponding to the insertion of Alu, SVA, and LINE1 mobile elements were identified at approximately 300 bp, 2 kb, and 6 kb, respectively (**Fig. 1d**). These SV patterns were consistent with previous studies.

Regarding the functional prediction of SVs, a significant proportion of SVs were located in intergenic (57.32%) or intronic regions (36.62%; **Fig. 1e**). Only 6.06% of SVs breakpoints intersected with functional elements, including exons (n = 3381), predicted loss-of-function (pLoF; n = 1895), copy-gain of entire genes (CG; n=1170) intragenic exonic duplication (IED; n=1308), and promoters (n = 655). On average, each genome harbored a mean of 173.96 SVs that altered the functions of 213 genes (121.37 pLoF affected 122.7 genes, 26.09 CG affected 65.4 genes, and 25.69 IED affected 25.1 genes; **Fig. 1f**), indicating that approximately 1.1 % of human protein-coding genes per individual could experience functional abnormalities due to SVs.

To ascertain whether the SVs identified in this study had been documented previously, we compared it with five publicly available SV databases, namely gnomAD[32], Audano et al., 2019[36], the Humen Gnome structural variation Consortium(HGSVC2)[37], Wu et al.[28], and dbVar[38] (accessed on September 30, 2023). Initially, we ensured that the SV coordinates in these databases were converted to GRCh38 to align with our dataset. An SV in our study was considered previously reported if the overlap with SVs from published datasets was equal to or exceeded 50%. Finally, our dataset exhibited the greatest number of overlapped SVs (48,027, overlapping rate 34.58%; **Fig. 1g**) with the dataset constructed by Wu et al., which was based on the long-read WGS results from 405 Chinese individuals. The shared ancestry of all Chinese individuals likely contributed to this substantial overlap. Furthermore, a significant number of overlapped SVs were also detected in gnomAD (43,755; 31.51%) and dbVar (40,206; 28.95%) datasets, two commonly used reference dataset known for their diverse ethnic populations' representations. In contrast, the overlap with HGSVC2 (25,643; 18.47%) and Audano et al. datasets (19,231; 13.85%) was relatively lower. Overall, 49.57% (68,830/138,859) of the SVs discovered in our study were novel and not previously documented (**Fig. 1g**). These novel SVs were characterized by a higher fraction of insertions ($p < 2.2\times10^{-16}$, fisher exact test), particularly in intergenic and intronic regions (both $p < 2.2\times10^{-16}$, fisher exact test; **Fig. 1h)**. Additionally, they showed a lower frequency of overlaps with functional elements, affecting an average of 20.61 SV-altered genes per genome, including 6.95 pLoF, 2.24 CG, and 11.41 IED (**Fig. 1i**).

**Associations of SVs with the gut microbiome**

After quality control during SV calling, 1,406 of the 1,839 samples had fecal shotgun metagenomics sequencing data available. A microbial genome-wide association study (mbGWAS) was conducted on 22,519 common high-quality SVs (MAF ≥ 1%) and 616 microbial features comprising 517 gut microbial taxa and 99 gut metabolic modules (GMMs) present in over 10% of individuals **(Supplementary Table 2)**. A total of 30 SVs (DEL = 16, INS = 7, DUP = 6, INV=1) were identified to be associated with gut microbial features with genome-wide significance ($p < 2.22 \times 10^{-6} = 0.05/22,519$; **Fig. 2a; Supplementary Table 3**). The genomic inflation factor (λ) ranged from 0.84 to 1.33 with a median value of 0.98 (**Fig. 2b**), indicating no obvious evidence of inflation except for specific mbGWAS tests. Only one association achieved the study-wide significance level ($p < 3.60 \times 10^{-9}$, adjusting for 22,519 SVs and 616 microbial features).

The most significant association was observed for a 6.5kb deletion (chr5:79657532-79664046) within the intron region of the gene *TENT2*, which was positively correlated with the relative abundance of the species *Coprobacillus sp. 29_1* ($\beta = 0.158$, $p = 2.50 \times 10^{-9}$; **Fig. 2c**). Carriers of this SV exhibited significantly higher mean relative abundances of *Coprobacillus sp. 29_1* (homozygous DEL: 0.15%; heterozygous DEL: 0.024%) than the non-carriers (0.015%; **Fig. 2d**). This GWAS test exhibited no inflation with a λ of 0.87. The identified SV had a MAF of 0.014 in this cohort and was specific to East Asiana (MAF=0.028 for ASN; MAF=0 for other populations) according to the 1000 Genomes database[39]. Further analysis revealed that this SV was correlated with concentrations of glycine ($p = 0.015$), ethanol ($p = 0.022$), monocytes ($p = 0.027$) and albumin ($p = 0.028$) by investigating its associations with blood parameters as well from this cohort (**Supplementary Fig. 5**). Interestingly, the species *Coprobacillus sp. 29_1* associated with the SV also showed correlation with the monocytes' concentration, suggesting potential interactions among the three. By calculating pairwise linkage disequilibrium (LD) between this SV and its neighboring SNPs, we found this SV was in a strong LD with the SNP chr5:79674158_C/T ($r^2 = 0.973$; **Fig. 2c**), which was also resided in the intronic region of *TENT2* and showed a significant association with *Coprobacillus sp. 29_1* ($\beta = 0.143$, $p = 2.18 \times 10^{-7}$). Consistent with the SV, this SNP had a MAF of 0.013 in this cohort and 0.027 in the ASN population, but was absent in other populations from the 1000 Genomes database. This SNP was identified as a susceptibility mutation for schizophrenia[40], and consistently *Coprobacillus sp. 29_1* has been reported to be enriched in the schizophrenia patients[11]. Due to the strong LD

between the SV and the SNP, the association with *Coprobacillus sp. 29_1* became unsignificant after conditioning on either of them. Both the SV and the SNP were located in the intronic region of gene *TENT2* that is well known to regulate miRNA stability and abundance via diverse mechanisms[41]. We hypothesize that the SV or the SNP may affect the gene expression of *TENT2*, potentially influencing immune function and gut homeostasis.

In addition to the study-wide significant signal, 22 SVs were found to be associated with microbial taxa at genome-wide significance (**Supplementary Table 3**). Among them, three SVs lied in the genes that were extremely intolerant to pLoF variants with pLI ≥ 0.99 as annotated by the AnnotSV tool. Specifically, a 61 bp duplication within the *CDH8* gene was negatively associated with the abundance of *Streptococcus sanguinis* ($\beta$ = -0.137, $p = 3.37 \times 10^{-7}$), a predominant bacterium in the human oral cavity known to be linked with the development of infective endocarditis[42]. Similarly, a 108 bp duplication in the *ANKRD11* gene was negatively associated with the abundance of *Turicibacter* ($\beta$ = -0.133, $p = 4.91 \times 10^{-7}$). The SV was overlapped with pathogenic loss genomic regions of *ANKRD11* that caused KBG syndrome, a disease characterized by intellectual disability, skeletal malformations, and macrodontia[43]. *Turicibacter* has been reported to be a highly heritable taxon in both human and mouse genetic studies[12,44,45], supporting the association between SV and *Turicibacter* abundance found in this study. Conversely, a 751 bp deletion in the *GRID2* was positively associated with the presence of *Eubacterium cellulosolvens* ($\beta$ = 0.755, $p = 6.85 \times 10^{-7}$), an anaerobic cellulolytic bacterium in the gut. The *GRID2* gene encodes the glutamate receptor channel delta-2 subunit and its deletion led to a recessive syndrome of cerebellar ataxia and tonic upgaze in humans[46].

In addition to the three SVs within disease-associated genes, several SVs were found to exhibit significant effects on potential probiotics that contributed to the host health. For example, a duplication event in the *LOC107985978* gene on chromosome 7 (SV length: 68 bp) was positively associated with the abundance of *Roseburia intestinalis* ($\beta$ = 0.139, $p = 2.20 \times 10^{-7}$), a promising probiotic known for its anti-inflammatory properties by producing butyrate[47,48]. An insertion on chromosome 15 involving an ALU element (SV length: 262 bp) demonstrated a significantly negative correlation with an emerging probiotics *Parabacteroides distasonis*[49] ($\beta$ = -0.137, $p = 2.51 \times 10^{-7}$).

Not only the microbial taxa, seven associations were identified for the GMMs or called microbial pathways. For instance, the glyoxylate bypass pathway (MF0063) was negatively associated with an insertion on chromosome 2 (SV length: 111 bp, $\beta$ = -0.147, $p = 2.92 \times 10^{-8}$). The pyruvate dehydrogenase complex (MF0072) exhibited a negative association with a deletion on chromosome 13 (SV length: 234 bp, $\beta$ = -0.132, $p = 3.26 \times 10^{-7}$). The pectin degradation II pathway (MF0004) exhibited a negative association with a deletion on chromosome 9 (SV length: 82 bp, $\beta$ = -0.131, $p = 5.19\times 10^{-7}$). Notably, all the SVs associated with the microbiome were located in the intronic and intergenic noncoding regions, except an inversion of 4.78Mb spanning 14 genes, consistent with previous findings in the SNP-based mbGWAS[50].

AnnotSV[51-53] was employed to annotate the 30 microbiome-associated SVs, resulting in the identification of 24 genes that harbored these SVs. Subsequently, gene enrichment analyses were conducted on these 24 genes. Gene Ontology (GO) enrichment analysis revealed 10 significantly enriched GO terms ($p$.adjust < 0.05), including one biological process (BP), six cellular component (CC), and one molecular function (MF) (**Supplementary Fig. 6a**; **Supplementary Table 5**). The enriched gene functions were predominantly related to the structure and functions of neuronal synapses, encompassing synaptic membrane, synaptic cleft, sodium-independent organic anion transport, sodium-independent organic anion transmembrane transporter activity, postsynaptic specialization membrane, postsynaptic density membrane, glutamatergic synapse, and excitatory synapse. Additionally, Kyoto Encyclopedia of Genes and Genomes (KEGG) enrichment analysis indicated significant enrichment of these genes in four pathways, namely nicotinate and nicotinamide metabolism, long-term depression, the peroxisome, and the phosphatidylinositol signaling system (**Supplementary Fig. 6b**; **Supplementary Table 6**). These findings suggested a potential pivotal role of microbiome-associated SVs in neurotransmission, ion transport, and cell signaling pathways.

**Conditional analyses of microbiome-associated SVs adjusting for SNPs/indels**

To further investigate the independence of the identified microbiome-associated SVs from nearby SNPs in influencing changes of microbial features, pairwise LD between SVs and their neighboring SNPs within the ±500kbp flanking region of SVs were

calculated. We found that 8 out of the 30 microbiome-associated SVs exhibited at least moderate LD ($r^2 \geq 0.5$) with one SNP or indel associated with the same microbial feature (**Fig. 3a**; **Supplementary Table 3-4**). Subsequently, conditional analyses were performed for each SV, adjusting for the tagging SNP that showed the strongest LD with the SV. These analyses confirmed that 8 SV-microbiome associations were no longer significant after adjusting for the SNP/indel at the same locus ($p > 0.01$; **Fig. 3b**), while the remaining 22 SVs maintained their significance. Notably, 11 of these 22 SVs retained genome-wide significance following conditional analyses ($p < 2.2\times10^{-6}$). These independent SV signals included two SVs potentially linked to probiotics—*Roseburia intestinalis* and *Parabacteroides distasonis*. These findings indicated that the majority of SVs (73%) rather than nearby SNPs were the primary causal agents driving changes in microbial abundance.

**Associations of SVs with blood metabolites**

We next conducted the GWAS for 22,519 common SVs and 121 blood metabolic traits. A total of 48 associations involving 33 SVs (DEL = 11, INS = 14, DUP = 8) reached genome-wide significance ($p < 2.2\times10^{-6} = 0.05/22519$; **Fig. 4a**; **Supplementary Table 7**). Among these, 17 associations reached study-wide significance ($p < 1.835\times10^{-8}$, adjusting for 22,519 SVs and 121 blood metabolite traits). The genomic inflation factor $\lambda$ was calculated, with a median value of 1 (ranging from 0.80 to 1.33; **Supplementary Fig. 7**).

The strongest association signal was observed for a deletion on chromosome 16 (chr16:165396-184700; SV length: 19,304 bp) spanning the *HBA1*, *HBA2*, *HBM*, and *HBQ1* genes, known as the widely reported Southeast Asian deletion ($--^{SEA}$) that is predominantly distributed and associated with anemia in southern China and Southeast Asia[54,55]. In the Chinese population of the study, the MAF of the SEA deletion was found to be 0.01. Consistently, the deletion was mainly detected in the East Asian (ASN, MAF=0.019) and South Asian (SAN, MAF=0.013) population in the 1000 Genomes dataset. The deletion showed remarkably significant associations with nine blood metabolic traits, in particularly with mean corpuscular volume (MCV, $\beta = -0.570$, $p = 1.22\times10^{-91}$), mean corpuscular hemoglobin (MCH, $\beta = -0.522$, $p = 4.19\times10^{-76}$), mean corpuscular hemoglobin concentration (MCHC, $\beta = -0.319$, $p = 4.31\times10^{-29}$), and red blood cell distribution (RBC, $\beta = -0.198$, $p = 2.43\times10^{-11}$; **Fig. 4**; **Supplementary Table**

**7**). Beyond its established correlations with blood cell parameters, the deletion was also observed to be associated with blood microelement levels. Carriers of the deletion exhibited elevated zinc and copper concentrations, while levels of magnesium, iron, and manganese were decreased compared to non-carriers (**Fig. 4b**).

In addition to the 16:165396-184700 deletion, a 114 bp duplication on chromosome 9 (chr9: 97255555-97255669) within the *SUGT1P4-STRA6LP-CCDC180* gene was also identified to be associated with MCV (β= -0.174, $p = 7.89\times10^{-9}$) and MCH (β= -0.174, $p = 7.89\times10^{-9}$) levels. This DUP had a MAF of 0.0125 in this study and has not been previously reported.

Among the total 48 genome-wide associations, cystine, previously reported as the most heritable metabolite in Chinese[56], exhibited the highest number of associated SVs, with 16 SVs found to be linked to it (**Fig. 5a**). Three SVs reached study-wide significance, including a 9.2kb deletion on chromosome 5 (5:46048650-46057870; β= -0.163, $p = 6.47\times10^{-10}$) and two insertions on chromosome 4 (β= -0.161, $p =2.83\times10^{-9}$) and 12 (β= -0.161, $p = 2.83\times10^{-9}$), respectively (**Supplementary Table 7**).

The results of GWAS and LD analysis revealed that three out of the 33 SVs appeared weaker associations with respective metabolites compared to neighboring SNPs and could be tagged by neighboring SNPs with $r^2$ >0.5 (**Supplementary Fig. 8**). Conditional analysis further confirmed the three SVs' associations with metabolites were attenuated even not significant after adjusting for neighboring SNPs. For example, the *HBA1*/*HBA2*/*HBM*/*HBQ1* deletion was in moderate LD with the lead SNP chr16:199621 across nine metabolic traits ($r^2$=0.76). After conditioning on the SNP, the association of the deletion with these traits was notably weakened, although it remained statistically significant for seven of them ($p$<0.01; **Supplementary Table 7**), highlighting the significance of this SV in influencing host metabolic processes that are not completely accounted for by nearby SNPs. Furthermore, a 64bp insertion (chr19: 15866773- 15866783) associated with the vitamin K concentration was in strong LD with its tagging SNP ($r^2$=0.94), while a ~6kb insertion (chr12: 20861159-20861190) associated with the direct bilirubin level was in moderate LD with its tagging SNP ($r^2$=0.76). These associations of two insertions with metabolites were not significant after adjusting for neighboring SNPs. Apart from these three SVs, the remaining 30

SVs continued to exhibit significant links with their respective metabolites after the conditional analysis, underscoring the potential driven and regulatory roles of these SVs in blood metabolic traits (**Supplementary Table 7-8**).

The GO enrichment analysis of gene sets in close proximity to significant SVs identified 26 BP, 16 CC, and 30 MF terms (**Fig. 5b; Supplementary Table 9**). The enriched gene sets predominantly featured biological process pathways encompassing gas transport, detoxification and redox, protein and receptor transport, metabolism, and degradation, indicating that SVs associated with blood metabolites play a pivotal role in these biological processes. Additionally, KEGG enrichment analysis revealed a notable enrichment of the gene sets in pathways associated with infectious diseases (e.g., African trypanosomiasis, malaria), bile secretion, and glycosylation-related metabolic pathways (**Fig. 5c; Supplementary Table 10**), implying a crucial role played by SVs located near these genes in these metabolic pathways.

**Replication of previously reported metabolites-associated SVs**

We investigated the previously reported metabolites-associated SVs to determine their replication in our study. Out of a total of 58 autosomal SVs identified from previous studies[26-28], 33 SVs were detected in our samples, with 16 of them showing associations with metabolites at a $p < 0.05$ **(Supplementary Table 11-13**). Notably, following a stringent Bonferroni correction threshold of 0.00152 (0.05/33), three SVs remained statistically significant. The most robust signal was observed for the *HBA1*/*HBA2*/*HBM*/*HBQ1* (16:165396-184701) SV, which exhibited associated with MCV/MCH that were confirmed by our study, the NHLBI TOPMed program and the study by Wu et al. Additionally, the SV within the growth hormone receptor (GHR) gene, previously linked to small round epithelial cell (SRC) count in the study by Wu et al, was found to be associated with multiple metabolites, including cystine, aspartic acid, and glutamic acid in our investigation. Moreover, the duplication involving the T cell receptor alpha variable (TRAV) genes, known to be associated with C-reactive protein (CRP) levels in the study by Chen et al, was also correlated with valine levels in our study. These replicated associations across different studies underscore the importance of some specific SVs in human metabolism, emphasizing the need for further validation in larger populations to confirm additional potential associations and advance our understanding in this domain.

**Host SVs associated with both microbiome and metabolites help understand their interactions**

Further, we investigated the potential contribution of host SVs to the intricate interactions between gut microbiome and blood metabolites. Initially, we observed that host SVs showed pleiotropic associations with both microbial features and plasma metabolites, demonstrating significant p-values reaching genome-wide significance ($p < 2.22 \times 10^{-6}$) for one phenotype and $p < 0.05$ for the other. Specifically, out of the 30 SVs significantly linked to the gut microbiome, 29 were found to be correlated with at least one blood metabolite (**Fig. 6a**; **Supplementary Table 14**). Similarly, among the 33 SVs significantly associated with blood metabolites, 31 were also correlated with at least one gut microbial feature (**Fig. 6b**; **Supplementary Table 15**).

Next, we directly calculated the phenotypic correlations between gut microbial features and blood metabolic traits. This approach resulted in the identification of 21 "microbial feature - metabolic trait" pairs meeting stringent significance criteria (associated the SV with $p<2.22 \times 10^{-6}$ for microbiome, $p<0.05$ for the metabolic trait, and $p<0.05$ for correlation between them; **Supplementary Table 14**). For example, a deletion on chromosome 8 (SV length: 141 bp) was significantly associated with both *Clostridium ramosum* ($\beta = 0.131$, $p = 7.47\times10^{-7}$) and serum uric acid ($\beta = 0.073$, $p = 1.52\times10^{-3}$). Moreover, a significant association was observed between *Clostridium ramosum* and serum uric acid ($\beta = 0.060$, $p = 3.61\times10^{-3}$; **Fig. 6c**). Another instance highlighted an insertion on chromosome 5 (SV length: 96 bp) significantly linked to both *Citrobacter* ($\beta = -0.129$, $p = 1.33\times10^{-6}$) and 1-methylhistidine ($\beta=-0.076$, $p = 4.22\times10^{-3}$), unveiling intricate relationships within *Citrobacter* and 1-methylhistidine (correlated $\beta = 0.048$, $p = 0.023$).

Likewise, we also identified 325 "metabolic trait - microbial feature" pairs that met the significance criteria (associated the SV with $p<2.22 \times 10^{-6}$ for metabolic trait, $p<0.05$ for the microbial feature, and $p<0.05$ for correlation between them; **Supplementary Table 15**). For example, the *HBA1*/*HBA2*/*HBM*/*HBQ1* deletion (chr16:165396-184700_DEL) significantly associated with nine blood metabolites such as MCHC and zinc were also linked to the relative abundance of the microbial pathway MF0064: the triacylglycerol degradation ($\beta = -0.082$, $p = 6.47\times10^{-10}$). A significant association was

observed between MCHC and MF0064: the triacylglycerol degradation ($\beta = 0.075$, $p = 2.85\times10^{-3}$; **Fig. 6d**). The significant correlation between zinc and MF0064: the triacylglycerol degradation was also observed ($\beta = -0.039$, $p = 4.95\times10^{-2}$; **Fig. 6e**). These results indicated a potential regulatory network involving these microbial and metabolic components, underscoring the importance of considering SVs in the context of microbial/metabolic associations.

To infer causal relationships, we utilized the SVs as instrumental variables (IVs) in a Mendelian randomization (MR) analysis. This approach revealed 24 significant causal relationships involving 21 microbial traits and 13 metabolic traits **(Supplementary Table 16**). Observational correlation and MR analysis consistently confirmed the causal effect of *Clostridium ramosum* on increased serum uric acid (**Fig. 6c)**, as well as *Citrobacter* on increased 1-methylhistidine. Morevover, blood MCHC, zinc, and manganese showed positive causal effects on the microbial pathway MF0064: the triacylglycerol degradation **(Fig. 6d-e)**. Additionally, tyrosine was found to be causally correlated with abundances of diverse gut microbiota, including *Salmonella enterica*, *Bacteroides intestinalis*, MF0052:arginine degradation II, Gammaproteobacteria, *Providencia rettgeri*, MF0093:propionate production I, and Enterobacteriaceae. These results highlight how host SVs could genetically determine the levels of blood metabolites and gut microbiome, even when the effect of one phenotype was mediated by the abundance of the other phenotype, facilitating a deep understanding of the interactive mechanisms shaping these biological phenotypes.

## Discussion

This study represents a comprehensive investigation into the role of SVs in the gut microbiome, blood metabolites and their interactions. Through high-depth whole-genome sequencing of 2,002 individuals, we identified 138,859 high-confidence SVs, nearly half of which were novel. The association analysis revealed 30 significant links between SVs and microbial taxa/pathways, as well as 48 significant associations between SVs and blood metabolites. Among these, 18 reached the study-wide significance. These findings highlight the intricate interaction between host genetic variation and the gut microbiome and metabolites, emphasizing the critical role of SVs in this process. This comprehensive SV dataset serves as a valuable genomic resource for the Chinese population and can function as a reference panel for SVs imputation in

GWAS, offering broad utility for future phenotype association studies, including those focusing on diseases.

The study revealed a strong association between specific SVs, particularly a deletion in the *TENT2* gene, and the relative abundance of *Coprobacillus sp. 29_1*. The *TENT2* gene is required for the mono-adenylation of certain miRNAs, such as the liver-specific miRNA-122, which is involved in the regulation of fatty acid homeostasis[57,58]. Existing literature has indicated the significant role of host miRNAs in modulating the gut microbiota[59]. *Coprobacillus* has been reported to be less abundant and could be a protective species to the psoriasis and psoriatic arthritis disease[60-62]. Previous studies have shown that individuals with high *AMY1* copy numbers (*AMY1-CN*) levels may promote the enrichment of *Ruminococcaceae* microbes (including *Ruminococcus* and *Oscillospira*) by consuming a diet rich in resistant starch, facilitating the efficient fermentation of resistant starch and positively impacting host health[25]. Our analysis identified nine SVs in the *AMY (AMY1, AMY2A, and AMY2B)* gene regions, with one spanning *AMY2A* (DUP, chr1:103611001-103620001), significantly associated with *Ruminococcaceae* ($\beta$ = -0.054, $p$ = 0.043). Additionally, a deletion near the *AMY* gene region (DEL, chr1:102630524-102630828) was identified as significantly negatively correlated with *Ruminococcus champanellensis* ($\beta$ = -0.111, $p = 1.74 \times 10^{-5}$) and *unclassified Ruminococcaceae bacterium_D16* ($\beta$ = -0.097, $p = 2.04 \times 10^{-4}$). These results supported the correlation between SV of *AMY* gene region and *Ruminococcaceae*, highlighting the role of microbiota in the human genetic adaptation[63].

Among the "SV-blood metabolite" associations, the most significant were observed for a 19kb deletion in the *HBA1/HBA2/HBM/HBQ1* gene region. The deletion as the well-known SEA variant exhibited a "thalassemia-like" pattern of red blood cell phenotypic associations, characterized by lower MCH, MCV and RBC. These findings were consistent with previous reports that this deletion is a key SV leading to alpha-thalassemia and linking to blood cell traits[27,28,64]. In addition to confirming associations with previously reported phenotypes (MCV, MCH, MCHC, and RBC), our findings revealed novel correlations with trace elements such as copper, zinc, and iron, underscoring this region's potential utility in disease screening and diagnosis. Beyond the *HBA1/HBA2/HBM/HBQ1* gene region, other associations were partially validated.

One study has reported that recurrent exon deletions in the *HP* (Haptoglobin) gene contribute to lower cholesterol levels[65]. We identified a deletion in the *HP* gene (DEL, chr16:72049453-72076286) significantly associated with total cholesterol (TC, $\beta$ = 0.061, $p$ = 0.04595). We also found an insertion in the *TOX2* gene (INS, chr20:44061952-44061987) significantly associated with TC ($\beta = 0.130$, $p = 2.04 \times 10^{-5}$), LDLC ($\beta = 0.118$, $p = 8.44 \times 10^{-5}$), and HDLC ($\beta = 0.056$, $p = 0.044$). The *TOX2* gene encodes a transcription factor involved in immune regulation[66]. The cholesterol and low-density lipoproteins are strongly linked to systemic inflammation[67,68]. This suggests that this SV may influence systemic inflammation and immune function by regulating blood lipid levels, requiring further analysis to clarify the mechanism of this association.

A noteworthy outcome of our study is that the majority of SVs appear to exert a dominant influence on microbial abundances and metabolic phenotypes, whereas the effects of nearby SNPs appear to be relatively limited. Traditional genome-wide association studies (GWAS) have primarily focused on the role of SNPs, however, many diseases such as rare and neurodevelopmental disorders[69-71] have been shown to be caused by SVs. Our study emphasizes the importance of SVs in the gut microbiome and associated metabolite changes, suggesting that future research should not exclusively concentrate on SNP-centric GWAS. Furthermore, most SV loci were found to affect both blood metabolites and gut microbiota, revealing the important role of SVs in the interplay between microbiota and blood metabolites. Previous research has established significant observational correlations between the microbiome and host metabolism[72-74], but our study highlights the crucial role of host genetics at the SV level within this context.

Despite providing valuable insights into SV-microbiota-metabolite interactions, our study has several limitations. Although our sample size is relatively large, particularly for microbiome SV GWAS, further studies are needed in an independent cohort or broader populations to ensure the generalizability of our findings. Moreover, the functional mechanisms of SVs remain incompletely understood. To gain deeper insights into how SVs influence the microbiome and regulate host metabolism, additional research is required using mouse models or functional experiments. As the number of reliable catalogs of SV loci continues to grow, we will gain deeper insights into the

impact of host SVs on the gut microbiome and blood metabolites, and a more nuanced understanding of the relationship between the gut microbiota, blood metabolites, and the host's physiological state. As more robust genetic variants are identified, future studies can further explore the causal relationships between microbiota and metabolites, thereby elucidating their potential roles in host health and disease.

In summary, this study has established a reference SV dataset for the Chinese population and has presented compelling evidence regarding SV associations with the gut microbiome and blood metabolites, laying the groundwork for future investigations and enriching our knowledge of human health and disease.

## Methods

### Study cohort and samples

Samples used in this study were obtained from the 4D-SZ omics-cohort, a cohort that has been described elsewhere[14,19,20,29-31]. In the year 2017, a total of 2002 individuals provided blood samples, and 1539 of these individuals also provided matched fecal samples as part of the annual health check program. The blood samples underwent high-depth whole genome sequencing and blood metabolic traits testing, whereas the fecal samples were subjected to shotgun metagenomic sequencing. The collection protocols for blood and stool samples, as well as the sequencing procedures, were consistent with those in earlier studies. Buffy coats were isolated from blood samples, and DNA was extracted using the HiPure Blood DNA Mini Kit (Magen, catalog no. D3111) according to the manufacturer’s protocol. Fecal samples were collected using the MGIEasy kit, and stool DNA was extracted using the MetaHIT protocol. Subsequently, DNA concentrations were quantified using Qubit (Invitrogen), and 200 ng of DNA from each sample was used for library preparation. Paired-end 100bp and single-end 100bp sequencing were performed for blood and stool samples, respectively, on the BGISEQ-500 platform[75].

Ethical approval for the study was obtained from the Institutional Review Boards (IRB) at BGI-Shenzhen, and all participants provided written informed consent.

### High-depth whole genome sequencing and SNP/indel detection

A total of 2,002 individuals in this study were sequenced to a mean sequencing depth

of 42× for the whole genome. The reads were aligned to the human reference genome GRCh38/hg38 using BWA (v.0.7.15)[76] with default parameters. The adapter sequences and bases with quality value below five were removed. The alignments were indexed in the BAM format using Samtools (v.0.1.18)[77] and PCR duplicates were marked for downstream filtering using Picardtools (v.1.62). The Genome Analysis Toolkit's (GATK v.4.3[78]) BaseRecalibrator created recalibration tables to screen known SNPs and insertions or deletions (INDELs) in the BAM files from dbSNP (v.150). GATKlite (v.2.2.15) was used for subsequent base quality recalibration and removal of read pairs with improperly aligned segments as determined by Stampy. GATK's HaplotypeCaller were used for variant discovery. GVCFs containing SNVs and INDELs from GATK HaplotypeCaller were combined (CombineGVCFs), genotyped (GenotypeGVCFs), variant score recalibrated (VariantRecalibrator) and filtered (ApplyRecalibration). During the GATK VariantRecalibrator process, we took our variants as inputs and used four standard SNP sets to train the model: (1) HapMap3.3 SNPs; (2) dbSNP build 150 SNPs; (3) 1000 Genomes Project SNPs from Omni 2.5 chip and (4) 1000 G phase1 high confidence SNPs. The sensitivity thresholds of 99.9% to SNPs and 99% to INDELs were applied for variant selection after optimizing for Transition to Transversion (TiTv) ratios using the GATK ApplyRecalibration command.

A stringent inclusion threshold for SNP/INDEL variants was established: (i) mean depth >8×; (ii) Hardy-Weinberg equilibrium (HWE) $P > 10^{-5}$; and (iii) genotype calling rate > 98%. Furthermore, sample criteria were as follows: (i) mean sequencing depth > 20×; (ii) variant calling rate > 98%; (iii) no population stratification by performing principal components analysis (PCA) analysis implemented in PLINK (v1.9) [79] and (iv) excluding related individuals by calculating pairwise identity by descent (IBD, Pi-hat threshold of 0.1875) in PLINK. Only 10 samples were removed in quality control filtering. After variant and sample quality control, 1,992 individuals with 8.5 million common (MAF ≥ 1%) SNP/indel variants were left for association analyses.

**SV detection**

Due to the complexity of SV detection from short-read sequencing data, use of multiple SV calling tools is a common practice to promote accuracy and sensitivity. For SV detection, a pipeline was designed according to SV-Adjudicator[33] (https://github.com/talkowski-lab/SV-Adjudicator) and GATK-SV cohort mode (https://github.com/broadinstitute/gatk-sv). In the pipeline, the BAM file obtained from

the preceding alignment and filtering process as its primary input. Subsequently, Manta (v1.6.0)[80], Wham (v1.7.0)[81], Svaba (v1.1.3)[82], and Delly (v0.8.7)[83] were run for SV detection, xTea[84] was run for mobile element insertion discovery, and cn.MOPS (v1.40.0)[85] and GATK gCNV[86] were run for CNVs calling (**Supplementary Fig. 3**). The algorithms were selected according to Kosugi et al[87]. Finally, the SV calls from the five algorithms and the CNV calls of each sample were standardized and integrated by GATK-SV pipeline. All computations were finished locally.

**Sample batching and quality control for SV**

Following the batching strategy delineated by Collins et al[32], all samples that passed the quality control (QC) were subdivided into 5 batches, with ~380 samples in each batch according to dosage score (WGD). The distribution of female and male samples in each batch was maintained at a ratio of approximately 1:1, ensuring balance across all batches.

For filtering after GATK-SV integration, outlier samples exhibiting either fewer or higher-than-average SV calls per contig for each caller, or samples manifesting autosomal aneuploidies based on the per-batch binned coverage of each chromosome, were excluded. Additionally, individuals with missing data or those who failed the preceding SNP/indel filtering were omitted. Finally, 1,839 samples were remained in the final SV callset.

**SV filtering**

To curate a high-quality SV dataset for subsequent genetic analyses, , a further filtration of SVs was conducted post-GATK-SV pipeline execution and sample quality assessment. SVs with quality scores (GQ) > 250 or marked as "PASS" were retained, while variants of type "BND" were excluded. The SVs with a genotyping rate >95% and Hardy-Weinberg equilibrium p value > $1x10^{-6}$ were kept. For GWAS analysis, only SVs with MAF >1% were retained, resulting in a final set of 22,519 SVs left for association analysis.

**SV Annotation**

The SVs that passed quality control were annotated using GATK SVAnnotate (GATK v4.6.0) for functional prediction. The protein-coding GTF file was downloaded from GENCODE (hg38.v37). Only protein-coding genes were kept for annotation. The BED

file of non-coding regions was downloaded from GATK-SV. AnnotSV (v3.3.8) was applied for additional SV annotation, utilizing the GRCh38 database build to incorporate information such as the pLI score of disrupted genes.

**Validation of SV using NA12878**

To validate the detection process of SV detection, the NA12878 human genome reference standard sequenced on BGISEQ-500 platform (https://db.cngb.org/search/experiment/CNX0094812/) was added as a demo into the cohort for GATK-SV integration. For evaluation of the SV detection, the final SV set of the demo was compared with the reference SV sets of NA12878 constructed with the datasets from the Database of Genomic Variants (http://dgv.tcag.ca/dgv/app/home) and the long read-derived SV data[35]. The evaluation was performed using EvalSVcallers (https://github.com/stat-lab/EvalSVcallers).

**Comparisons with published SV datasets**

We examined whether the SVs detected in this study have been reported in five publicly available SV databases, including gnomAD, Audano et al., 2019, HGSVC, Wu et al., and dbVar (spanning from 2018 to September 30, 2023). The gnomAD project is a high-coverage (average depth of 32X) short-read sequencing (SRS) dataset comprising 14,891 global samples. dbVar database catalogs SVs from multiple platforms. We first ensured that the coordinates of the SVs in these public databases were in GRCh38. Our strategy involved the utilization of the R package (v2.3.0) and a custom program to compare our identified SVs with those in the public databases, considering a reciprocal overlap rate of 50% or higher.

**Shotgun metagenomic sequencing and profiling**

For the fecal samples obtained from the SZ-4D cohort, DNA libraries were constructed and sequenced using the BGISEQ-500-DNA sequencer for subsequent metagenomic analysis. Raw data underwent quality control and adapter trimming through fastp (v0.23.2) software. To filter out human reads, the sequencing reads were aligned to the hg38 reference genome using SOAP2 (v2.22[88]) with an identity threshold of $\geq 0.9$. The gene profiles were generated by aligning high-quality sequencing reads to the integrated gene catalog (IGC) by using SOAP2 (identity $\geq 0.95$) as previously described[89]. The relative abundance profiles of phylum, order, family, class, genera and species were

determined from the gene abundances. To eliminate the influence of sequencing depth in comparative analyses, we downsized the unique IGC mapped reads to 20 million for each sample. The relative abundance profiles of gene, phylum, order, family, class, genus and species were determined accordingly using the downsized mapped reads per sample.

Gut metabolic modules (GMMs) characterize the bacterial and archaeal metabolism specific to the human gut, emphasizing anaerobic fermentation processes[90]. The current GMM set was developed through a comprehensive review of the literature and metabolic databases, including MetaCyc[91] and KEGG, followed by expert curation to define modules and alternative pathways. Ultimately, we identified 616 common microbial taxa and GMMs present in at least 10% of the samples.

**Microbiome association analysis**

We examined the relationship between host genetic variations and gut taxa/GMMs by utilizing linear or logistic models based on the abundance of each taxon/GMM. The abundance of taxon/GMM with an occurrence rate exceeding 95% in the cohort was log-transformed, and outliers (deviating over 4 standard deviations from the mean) were excluded to ensure reliable quantitative trait analysis. Alternatively, the taxon/GMM was categorized into presence/absence pattern to mitigate zero inflation issues, treating the abundance as a dichotomous trait. Subsequently, for SNP/indel and SV identified in this cohort, we conducted a standard single variant-based mbGWAS analysis using PLINK (v1.9) [79] with a linear model for quantitative traits or a logistic model for dichotomous traits. Considering the influence of diet and lifestyle on microbial characteristics, we incorporated age, gender, BMI, defecation frequency, stool form, 12 diet/lifestyle factors, along with the top four principal components as covariates for mbGWAS analysis.

**Metabolic trait profiling**

In this study, metabolic traits, including anthropometric characteristics and blood metabolites, were assessed for all participants during physical examinations. Anthropometric data, including height, weight, waist circumference, and hip circumference, were recorded by nurses, while age and gender were self-reported. Clinical evaluations, such as blood tests and urinalysis, were conducted by a certified physical examination organization. Blood amino acids were quantified using ultra-high

pressure liquid chromatography (UHPLC) coupled with an AB Sciex Qtrap 5500 mass spectrometer, utilizing electrospray ionization (ESI) in positive ion mode with 40 µl of plasma. Hormones were measured in a similar manner, with 250 µl of plasma and atmospheric pressure chemical ionization (APCI). Trace elements were analyzed using a 7700x ICP-MS (Agilent Technologies) equipped with octupole reaction system (ORS) technology to reduce spectral interferences, using 200 µl of whole blood. Water-soluble vitamins were assessed by UPLC coupled to a Xevo TQ-S Triple Quad mass spectrometer (Waters) with ESI in positive ion mode, utilizing 200 µl of plasma. Fat-soluble vitamins were measured with UPLC linked to an AB Sciex Qtrap 4500 mass spectrometer using APCI and 250 µl of plasma.

**Metabolites association analysis**

The log10-transformed median-normalized values of 121 anthropometric and metabolic traits were used as quantitative traits. Samples with missing values or values more than 4 standard deviations from the mean were excluded from the association analysis. Each of the SNP/indel or SV was independently tested using a linear model for quantitative traits in PLINK. Covariates included age, gender, and the top four principal components (PCs).

**Gene enrichment analysis**

The genes harboring significantly associated SVs were annotated using AnnotSV[51-53]. Gene Ontology (GO) and Kyoto Encyclopaedia of Genes and Genomes (KEGG) gene functional enrichment analysis of genes harboring significantly associated SVs were executed by using the R packages including clusterProfiler, enrichplot, ggplot2 and org.Hs.eg.db. A standardized metric ($p$-value < 0.05, Q-value < 0.2) was used to prioritize the top functional items and pathways. Biological process (BP), cellular component (CC), and molecular function (MF) were the three categories included in the GO analysis.

**Observational correlation analyses**

All microbial features and metabolic traits were transformed using log-transformed median-normalized function to reduce skewness of distributions. The observational correlations between them were evaluated by multivariable linear regression analysis while adjusted for age and gender. The beta coefficient and p-value were obtained.

**One-sample MR analysis.**

To explore potential causal relationships between microbial traits and metabolic characteristics within the same cohort, we conducted a one-sample bidirectional MR analysis in this cohort with both metabolite and microbiome data. We selected SV instruments based on a stringent genome-wide significance threshold ($p < 2.22 \times 10^{-6}$) and performed clumping with an LD $r^2 < 0.1$ to ensure independence among genetic variants for MR analysis. An unweighted polygenic risk score (PRS) was calculated for each participant based on independent genetic variants derived from GWAS data. For each SV, we coded the risk alleles as 0, 1, or 2, depending on the number of trait-specific risk alleles carried by the individual. Instrumental variable (IV) analyses were conducted using two-stage least squares (TSLS) regression. In the first stage, we assessed the association between the PRS and the observational phenotype using linear regression, from which we derived fitted values representing the predicted exposure. During this process, the *F*-statistics and variance explained by IVs were calculated. We demanded the *F*-statistics over 10 to ensure a strong IV for analysis. In the second stage, we regressed the outcome trait on the genetically predicted exposure from the first stage. Both stages were adjusted for potential confounders, including age, gender, and BMI. TSLS was performed using the 'ivreg' function from the AER package in R (v.1.2-9; https://www.rdocumentation.org/packages/AER/versions/1.2-9/topics/ivreg).

**Data Availability**

All summary statistics that support the findings of this study including the population SV dataset were available in the **Supplementary Tables**. The gut metagenomic sequencing data after removing host reads of 618 individuals as part of this study have been publicly available in the CNGB from https://db.cngb.org/search/project/CNP0000289/. All the metagenomics data, as well as the metabolites and individual-level host genetics data have been uploaded to the GSA database (https://ngdc.cncb.ac.cn/bioproject/browse/PRJCA005334). According to the Human Genetic Resources Administration of China regulation and the institutional review board of BGI-Shenzhen related to protecting individual privacy, these data are controlled-access and are available via an application on request. The datasets of common SVs are available at the following link: GnomAD SV:

https://datasetgnomad.blob.core.windows.net/dataset/release/4.1/genome_sv/gnomad.v4.1.sv.sites.vcf.gz, dbvar SV: https://gnomad.broadinstitute.org/, HGSVC SV: http://ftp.1000genomes.ebi.ac.uk/vol1/ftp/data_collections/HGSVC2/release/v1.0/integrated_callset/freeze3.sv.alt.vcf.gz, Wu et al SV: https://ftp.ncbi.nlm.nih.gov/pub/dbVar/data/Homo_sapiens/by_study/csv/all_variants_for_nstd212.csv.gz, Audano et al. 2019: http://ftp.1000genomes.ebi.ac.uk/vol1/ftp/data_collections/hgsv_sv_discovery/working/20181025_EEE_SV-Pop_1.

## Author Contributions

X.L and T.Z. conceived and organized this study. X.X., H.Y., Y.Z., W.L, X.J., and L.X. led the organization of the cohort, the sample collection, and the questionnaire collection. M.H. and H.L led the DNA extraction and sequencing. X.L and X.T. processed the whole genome data. L.Z., Y.J., and M.L. processed the metagenome data. X.L., X.T., and L.Z. performed the metagenome-genome-wide association analyses and Mendelian randomization analyses. X.L. wrote the raw manuscript. All authors contributed to data and texts in this manuscript.

## Competing interests

The authors declare no competing interest.

## Acknowledgments

We sincerely thank the support by the National Natural Science Foundation of China (No. 32200548) and the China National GeneBank. We thank all the volunteers for their time and for self-collecting the oral samples using our kit. The schematic workflow diagram of the study was drawn by Figdraw (https://www.figdraw.com).

## Reference

1 Liu, R. *et al.* Gut microbiome and serum metabolome alterations in obesity and after weight-loss intervention. *Nat Med* **23**, 859-868 (2017). https://doi.org:10.1038/nm.4358

2 Wu, C. *et al.* Obesity-enriched gut microbe degrades myo-inositol and promotes lipid absorption. *Cell Host & Microbe* **32**, 1301-1314.e1309 (2024). https://doi.org:10.1016/j.chom.2024.06.012

3 Qin, J. *et al.* A metagenome-wide association study of gut microbiota in type 2 diabetes.

*Nature* **490**, 55-60 (2012). https://doi.org:10.1038/nature11450

4 Mei, Z. *et al.* Strain-specific gut microbial signatures in type 2 diabetes identified in a cross-cohort analysis of 8,117 metagenomes. *Nature Medicine* **30**, 2265-2276 (2024). https://doi.org:10.1038/s41591-024-03067-7

5 Lloyd-Price, J. *et al.* Multi-omics of the gut microbial ecosystem in inflammatory bowel diseases. *Nature* **569**, 655-662 (2019). https://doi.org:10.1038/s41586-019-1237-9

6 Zheng, J. *et al.* Noninvasive, microbiome-based diagnosis of inflammatory bowel disease. *Nature Medicine* (2024). https://doi.org:10.1038/s41591-024-03280-4

7 Zhang, X. *et al.* The oral and gut microbiomes are perturbed in rheumatoid arthritis and partly normalized after treatment. *Nature Medicine* **21**, 895-905 (2015). https://doi.org:10.1038/nm.3914

8 Alpizar-Rodriguez, D. *et al.* Prevotella copri in individuals at risk for rheumatoid arthritis. *Ann Rheum Dis* **78**, 590-593 (2019). https://doi.org:10.1136/annrheumdis-2018-214514

9 Jie, Z. *et al.* The gut microbiome in atherosclerotic cardiovascular disease. *Nat Commun* **8**, 845 (2017). https://doi.org:10.1038/s41467-017-00900-1

10 Zhu, F. *et al.* Transplantation of microbiota from drug-free patients with schizophrenia causes schizophrenia-like abnormal behaviors and dysregulated kynurenine metabolism in mice. *Mol Psychiatry* (2019). https://doi.org:10.1038/s41380-019-0475-4

11 Zhu, F. *et al.* Metagenome-wide association of gut microbiome features for schizophrenia. *Nature Communications* **11**, 1612 (2020). https://doi.org:10.1038/s41467-020-15457-9

12 Goodrich, J. K. *et al.* Genetic Determinants of the Gut Microbiome in UK Twins. *Cell Host Microbe* **19**, 731-743 (2016). https://doi.org:10.1016/j.chom.2016.04.017

13 Goodrich, J. K., Davenport, E. R., Waters, J. L., Clark, A. G. & Ley, R. E. Cross-species comparisons of host genetic associations with the microbiome. *Science* **352**, 532-535 (2016). https://doi.org:10.1126/science.aad9379

14 Liu, X. *et al.* Mendelian randomization analyses support causal relationships between blood metabolites and the gut microbiome. *Nat Genet* **54**, 52-61 (2022). https://doi.org:10.1038/s41588-021-00968-y

15 Rühlemann, M. C. *et al.* Genome-wide association study in 8,956 German individuals identifies influence of ABO histo-blood groups on gut microbiome. *Nature genetics* **53**, 147-155 (2021). https://doi.org:10.1038/s41588-020-00747-1

16 Kurilshikov, A. *et al.* Large-scale association analyses identify host factors influencing human gut microbiome composition. *Nature genetics* **53**, 156-165 (2021). https://doi.org:10.1038/s41588-020-00763-1

17 Lopera-Maya, E. A. *et al.* Effect of host genetics on the gut microbiome in 7,738 participants of the Dutch Microbiome Project. *Nature Genetics* **54**, 143-151 (2022). https://doi.org:10.1038/s41588-021-00992-y

18 Qin, Y. *et al.* Combined effects of host genetics and diet on human gut microbiota and incident disease in a single population cohort. *Nature genetics* **54**, 134-142 (2022). https://doi.org:10.1038/s41588-021-00991-z

19 Liu, X. *et al.* A genome-wide association study for gut metagenome in Chinese adults illuminates complex diseases. *Cell Discovery* **7**, 9 (2021). https://doi.org:10.1038/s41421-020-00239-w

20 Liu, X. *et al.* Metagenome-genome-wide association studies reveal human genetic impact

on the oral microbiome. *Cell Discovery* **7**, 117 (2021). https://doi.org:10.1038/s41421-021-00356-0

21 Stankiewicz, P. & Lupski, J. R. Structural Variation in the Human Genome and its Role in Disease. *Annual Review of Medicine* **61**, 437-455 (2010). https://doi.org:https://doi.org/10.1146/annurev-med-100708-204735

22 D'Haene, E. & Vergult, S. Interpreting the impact of noncoding structural variation in neurodevelopmental disorders. *Genet Med* **23**, 34-46 (2021). https://doi.org:10.1038/s41436-020-00974-1

23 Fu, J. M. *et al.* Rare coding variation provides insight into the genetic architecture and phenotypic context of autism. *Nature genetics* **54**, 1320-1331 (2022). https://doi.org:10.1038/s41588-022-01104-0

24 Li, Y. *et al.* Patterns of somatic structural variation in human cancer genomes. *Nature* **578**, 112-121 (2020). https://doi.org:10.1038/s41586-019-1913-9

25 Poole, A. C. *et al.* Human Salivary Amylase Gene Copy Number Impacts Oral and Gut Microbiomes. *Cell Host Microbe* **25**, 553-564 e557 (2019). https://doi.org:10.1016/j.chom.2019.03.001

26 Chen, L. *et al.* Association of structural variation with cardiometabolic traits in Finns. *The American Journal of Human Genetics* **108**, 583-596 (2021). https://doi.org:https://doi.org/10.1016/j.ajhg.2021.03.008

27 Wheeler, M. M. *et al.* Whole genome sequencing identifies structural variants contributing to hematologic traits in the NHLBI TOPMed program. *Nature Communications* **13**, 7592 (2022). https://doi.org:10.1038/s41467-022-35354-7

28 Wu, Z. *et al.* Structural variants in the Chinese population and their impact on phenotypes, diseases and population adaptation. *Nature Communications* **12**, 6501 (2021). https://doi.org:10.1038/s41467-021-26856-x

29 Jie, Z. *et al.* A transomic cohort as a reference point for promoting a healthy human gut microbiome. *Medicine in Microecology* **8**, 100039 (2021). https://doi.org:https://doi.org/10.1016/j.medmic.2021.100039

30 Liu, X. *et al.* A genome-wide association study reveals the relationship between human genetic variation and the nasal microbiome. *Communications Biology* **7**, 139 (2024). https://doi.org:10.1038/s42003-024-05822-5

31 Liu, X. *et al.* Sex differences in the oral microbiome, host traits, and their causal relationships. *iScience* **26**, 105839 (2023). https://doi.org:10.1016/j.isci.2022.105839

32 Collins, R. L. *et al.* A structural variation reference for medical and population genetics. *Nature* **581**, 444-451 (2020). https://doi.org:10.1038/s41586-020-2287-8

33 Werling, D. M. *et al.* An analytical framework for whole-genome sequence association studies and its implications for autism spectrum disorder. *Nature genetics* **50**, 727-736 (2018). https://doi.org:10.1038/s41588-018-0107-y

34 Abel, H. J. *et al.* Mapping and characterization of structural variation in 17,795 human genomes. *Nature* **583**, 83-89 (2020). https://doi.org:10.1038/s41586-020-2371-0

35 Kosugi, S. *et al.* Comprehensive evaluation of structural variation detection algorithms for whole genome sequencing. *Genome Biology* **20**, 117 (2019). https://doi.org:10.1186/s13059-019-1720-5

36 Audano, P. A. *et al.* Characterizing the Major Structural Variant Alleles of the Human

Genome. *Cell* **176**, 663-675.e619 (2019). https://doi.org:10.1016/j.cell.2018.12.019

37 Ebert, P. *et al.* Haplotype-resolved diverse human genomes and integrated analysis of structural variation. *Science* **372**, eabf7117 (2021). https://doi.org:doi:10.1126/science.abf7117

38 Lappalainen, I. *et al.* dbVar and DGVa: public archives for genomic structural variation. *Nucleic acids research* **41**, D936-D941 (2012). https://doi.org:10.1093/nar/gks1213

39 Byrska-Bishop, M. *et al.* High-coverage whole-genome sequencing of the expanded 1000 Genomes Project cohort including 602 trios. *Cell* **185**, 3426-3440.e3419 (2022). https://doi.org:10.1016/j.cell.2022.08.004

40 Lam, M. *et al.* Comparative genetic architectures of schizophrenia in East Asian and European populations. *Nature genetics* **51**, 1670-1678 (2019). https://doi.org:10.1038/s41588-019-0512-x

41 Yang, A. *et al.* TENT2, TUT4, and TUT7 selectively regulate miRNA sequence and abundance. *Nature Communications* **13**, 5260 (2022). https://doi.org:10.1038/s41467-022-32969-8

42 Martini, A. M., Moricz, B. S., Woods, L. J. & Jones, B. D. Type IV Pili of Streptococcus sanguinis Contribute to Pathogenesis in Experimental Infective Endocarditis. *Microbiology Spectrum* **9**, e01752-01721 (2021). https://doi.org:doi:10.1128/Spectrum.01752-21

43 Sirmaci, A. *et al.* Mutations in ANKRD11 cause KBG syndrome, characterized by intellectual disability, skeletal malformations, and macrodontia. *Am J Hum Genet* **89**, 289-294 (2011). https://doi.org:10.1016/j.ajhg.2011.06.007

44 Benson, A. K. *et al.* Individuality in gut microbiota composition is a complex polygenic trait shaped by multiple environmental and host genetic factors. *Proc Natl Acad Sci U S A* **107**, 18933-18938 (2010). https://doi.org:10.1073/pnas.1007028107

45 Org, E. *et al.* Genetic and environmental control of host-gut microbiota interactions. *Genome research* **25**, 1558-1569 (2015). https://doi.org:10.1101/gr.194118.115

46 Hills, L. B. *et al.* Deletions in GRID2 lead to a recessive syndrome of cerebellar ataxia and tonic upgaze in humans. *Neurology* **81**, 1378-1386 (2013). https://doi.org:10.1212/WNL.0b013e3182a841a3

47 La Rosa, S. L. *et al.* The human gut Firmicute Roseburia intestinalis is a primary degrader of dietary β-mannans. *Nature Communications* **10**, 905 (2019). https://doi.org:10.1038/s41467-019-08812-y

48 Louis, P. & Flint, H. J. Formation of propionate and butyrate by the human colonic microbiota. *Environ. Microbiol.* **19**, 29-41 (2017). https://doi.org:https://doi.org/10.1111/1462-2920.13589

49 Zhao, Q. *et al.* Parabacteroides distasonis ameliorates hepatic fibrosis potentially via modulating intestinal bile acid metabolism and hepatocyte pyroptosis in male mice. *Nature Communications* **14**, 1829 (2023). https://doi.org:10.1038/s41467-023-37459-z

50 Markowitz, R. H. G. *et al.* Microbiome-associated human genetic variants impact phenome-wide disease risk. *Proc Natl Acad Sci U S A* **119**, e2200551119 (2022). https://doi.org:10.1073/pnas.2200551119

51 Geoffroy, V. *et al.* The AnnotSV webserver in 2023: updated visualization and ranking. *Nucleic acids research* **51**, W39-w45 (2023). https://doi.org:10.1093/nar/gkad426

52 Geoffroy, V. *et al.* AnnotSV and knotAnnotSV: a web server for human structural variations

annotations, ranking and analysis. *Nucleic acids research* **49**, W21-w28 (2021). https://doi.org:10.1093/nar/gkab402

53 Geoffroy, V. *et al.* AnnotSV: an integrated tool for structural variations annotation. *Bioinformatics* **34**, 3572-3574 (2018). https://doi.org:10.1093/bioinformatics/bty304

54 Qiu, Q. W. *et al.* Evidence of recent natural selection on the Southeast Asian deletion (--(SEA)) causing α-thalassemia in South China. *BMC Evol Biol* **13**, 63 (2013). https://doi.org:10.1186/1471-2148-13-63

55 Gao, Y. *et al.* A pangenome reference of 36 Chinese populations. *Nature* **619**, 112-121 (2023). https://doi.org:10.1038/s41586-023-06173-7

56 Liu, X. *et al.* Mendelian randomization analyses support causal relationships between blood metabolites and the gut microbiome. *Nature genetics* **54**, 52-61 (2022). https://doi.org:10.1038/s41588-021-00968-y

57 Warkocki, Z., Liudkovska, V., Gewartowska, O., Mroczek, S. & Dziembowski, A. Terminal nucleotidyl transferases (TENTs) in mammalian RNA metabolism. *Philos Trans R Soc Lond B Biol Sci* **373** (2018). https://doi.org:10.1098/rstb.2018.0162

58 Katoh, T. *et al.* Selective stabilization of mammalian microRNAs by 3' adenylation mediated by the cytoplasmic poly(A) polymerase GLD-2. *Genes Dev* **23**, 433-438 (2009). https://doi.org:10.1101/gad.1761509

59 Liu, S. *et al.* The Host Shapes the Gut Microbiota via Fecal MicroRNA. *Cell Host Microbe* **19**, 32-43 (2016). https://doi.org:10.1016/j.chom.2015.12.005

60 Scher, J. U. *et al.* Decreased bacterial diversity characterizes the altered gut microbiota in patients with psoriatic arthritis, resembling dysbiosis in inflammatory bowel disease. *Arthritis Rheumatol* **67**, 128-139 (2015). https://doi.org:10.1002/art.38892

61 Olejniczak-Staruch, I. *et al.* Alterations of the Skin and Gut Microbiome in Psoriasis and Psoriatic Arthritis. *Int J Mol Sci* **22** (2021). https://doi.org:10.3390/ijms22083998

62 Zou, X., Zou, X., Gao, L. & Zhao, H. Gut microbiota and psoriasis: pathogenesis, targeted therapy, and future directions. *Front Cell Infect Microbiol* **14**, 1430586 (2024). https://doi.org:10.3389/fcimb.2024.1430586

63 Suzuki, T. A. & Ley, R. E. The role of the microbiota in human genetic adaptation. *Science* **370** (2020). https://doi.org:10.1126/science.aaz6827

64 Ireland, J. H. *et al.* Detection of the (--SEA) double alpha-globin gene deletion by a simple immunologic assay for embryonic zeta-globin chains. *Am J Hematol* **44**, 22-28 (1993). https://doi.org:10.1002/ajh.2830440106

65 Boettger, L. M. *et al.* Recurring exon deletions in the HP (haptoglobin) gene contribute to lower blood cholesterol levels. *Nature genetics* **48**, 359-366 (2016). https://doi.org:10.1038/ng.3510

66 Seo, H. *et al.* TOX and TOX2 transcription factors cooperate with NR4A transcription factors to impose CD8<sup>+</sup> T cell exhaustion. *Proceedings of the National Academy of Sciences* **116**, 12410-12415 (2019). https://doi.org:doi:10.1073/pnas.1905675116

67 Tall, A. R. & Yvan-Charvet, L. Cholesterol, inflammation and innate immunity. *Nat Rev Immunol* **15**, 104-116 (2015). https://doi.org:10.1038/nri3793

68 Jukema, R. A., Ahmed, T. A. N. & Tardif, J.-C. Does low-density lipoprotein cholesterol induce inflammation? If so, does it matter? Current insights and future perspectives for

989 novel therapies. *BMC Medicine* **17**, 197 (2019). https://doi.org:10.1186/s12916-019-
990 1433-3
991 69 Mizuguchi, T. *et al.* A 12-kb structural variation in progressive myoclonic epilepsy was
992 newly identified by long-read whole-genome sequencing. *Journal of Human Genetics* **64**,
993 359-368 (2019). https://doi.org:10.1038/s10038-019-0569-5
994 70 Cen, Z. *et al.* Intronic pentanucleotide TTTCA repeat insertion in the SAMD12 gene causes
995 familial cortical myoclonic tremor with epilepsy type 1. *Brain* **141**, 2280-2288 (2018).
996 https://doi.org:10.1093/brain/awy160
997 71 Kaivola, K. *et al.* Genome-wide structural variant analysis identifies risk loci for non-
998 Alzheimer's dementias. *Cell Genom* **3**, 100316 (2023).
999 https://doi.org:10.1016/j.xgen.2023.100316
1000 72 Visconti, A. *et al.* Interplay between the human gut microbiome and host metabolism.
1001 *Nature Communications* **10**, 4505 (2019). https://doi.org:10.1038/s41467-019-12476-z
1002 73 Kinross, J. M., Darzi, A. W. & Nicholson, J. K. Gut microbiome-host interactions in health
1003 and disease. *Genome Medicine* **3**, 14 (2011). https://doi.org:10.1186/gm228
1004 74 Dekkers, K. F. *et al.* An online atlas of human plasma metabolite signatures of gut
1005 microbiome composition. *Nature Communications* **13**, 5370 (2022).
1006 https://doi.org:10.1038/s41467-022-33050-0
1007 75 Fang, C. *et al.* Assessment of the cPAS-based BGISEQ-500 platform for metagenomic
1008 sequencing. *Gigascience* **7**, 1-8 (2018). https://doi.org:10.1093/gigascience/gix133
1009 76 Li, H. & Durbin, R. Fast and accurate short read alignment with Burrows-Wheeler
1010 transform. *Bioinformatics* **25**, 1754-1760 (2009).
1011 https://doi.org:10.1093/bioinformatics/btp324
1012 77 Li, H. *et al.* The Sequence Alignment/Map format and SAMtools. *Bioinformatics* **25**, 2078-
1013 2079 (2009). https://doi.org:10.1093/bioinformatics/btp352
1014 78 McKenna, A. *et al.* The Genome Analysis Toolkit: a MapReduce framework for analyzing
1015 next-generation DNA sequencing data. *Genome research* **20**, 1297-1303 (2010).
1016 https://doi.org:10.1101/gr.107524.110
1017 79 Purcell, S. *et al.* PLINK: a tool set for whole-genome association and population-based
1018 linkage analyses. *Am J Hum Genet* **81**, 559-575 (2007). https://doi.org:10.1086/519795
1019 80 Chen, X. *et al.* Manta: rapid detection of structural variants and indels for germline and
1020 cancer sequencing applications. *Bioinformatics* **32**, 1220-1222 (2016).
1021 https://doi.org:10.1093/bioinformatics/btv710
1022 81 Kronenberg, Z. N. *et al.* Wham: Identifying Structural Variants of Biological Consequence.
1023 *PLoS Comput Biol* **11**, e1004572 (2015). https://doi.org:10.1371/journal.pcbi.1004572
1024 82 Wala, J. A. *et al.* SvABA: genome-wide detection of structural variants and indels by local
1025 assembly. *Genome research* **28**, 581-591 (2018). https://doi.org:10.1101/gr.221028.117
1026 83 Rausch, T. *et al.* DELLY: structural variant discovery by integrated paired-end and split-
1027 read analysis. *Bioinformatics* **28**, i333-i339 (2012).
1028 https://doi.org:10.1093/bioinformatics/bts378
1029 84 Chu, C. *et al.* Comprehensive identification of transposable element insertions using
1030 multiple sequencing technologies. *Nature Communications* **12**, 3836 (2021).
1031 https://doi.org:10.1038/s41467-021-24041-8
1032 85 Klambauer, G. *et al.* cn.MOPS: mixture of Poissons for discovering copy number variations

in next-generation sequencing data with a low false discovery rate. *Nucleic acids research* **40**, e69 (2012). https://doi.org:10.1093/nar/gks003

86 Van der Auwera, G. A. & O'Connor, B. D. *Genomics in the cloud: using Docker, GATK, and WDL in Terra*. (O'Reilly Media, 2020).

87 Kosugi, S. *et al.* Comprehensive evaluation of structural variation detection algorithms for whole genome sequencing. *Genome Biol* **20**, 117 (2019). https://doi.org:10.1186/s13059-019-1720-5

88 Li, R. *et al.* SOAP2: an improved ultrafast tool for short read alignment. *Bioinformatics* **25**, 1966-1967 (2009). https://doi.org:10.1093/bioinformatics/btp336

89 Li, J. *et al.* An integrated catalog of reference genes in the human gut microbiome. *Nat Biotechnol* **32**, 834-841 (2014). https://doi.org:10.1038/nbt.2942

90 Vieira-Silva, S. *et al.* Species-function relationships shape ecological properties of the human gut microbiome. *Nat Microbiol* **1**, 16088 (2016). https://doi.org:10.1038/nmicrobiol.2016.88

91 Caspi, R. *et al.* The MetaCyc database of metabolic pathways and enzymes and the BioCyc collection of Pathway/Genome Databases. *Nucleic acids research* **42**, D459-471 (2014). https://doi.org:10.1093/nar/gkt1103

## Graphic abstract

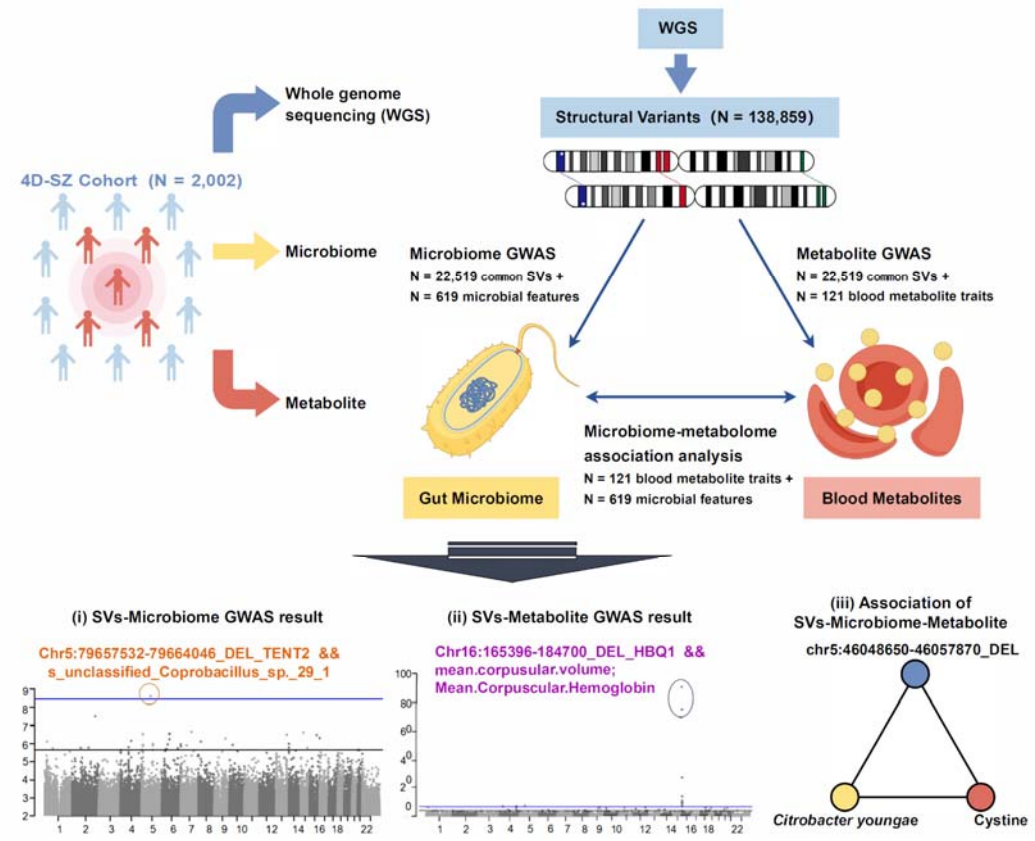

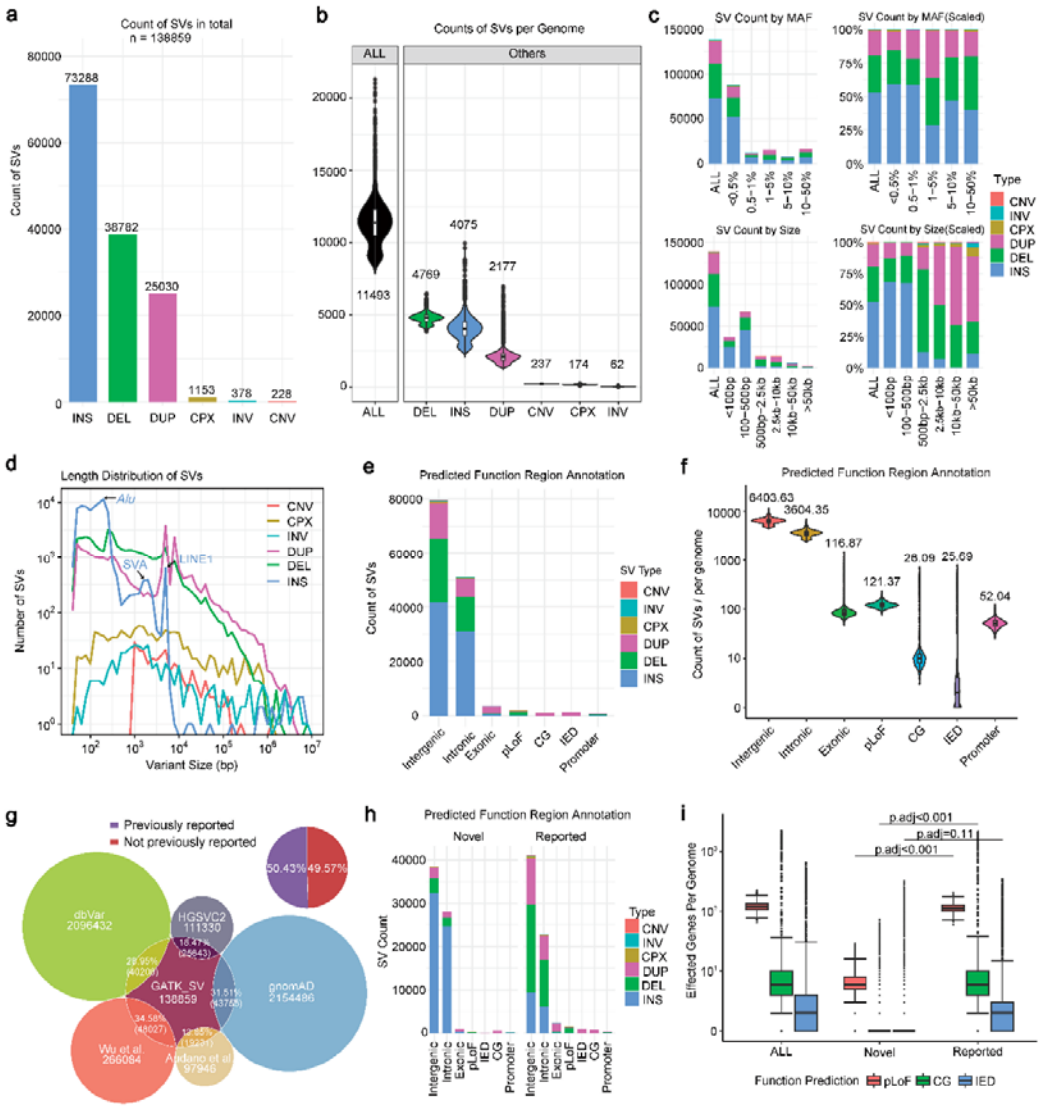


**Figure 1. Characteristics of the SVs discovered in this study (4D-SZ Cohort).**

(**a**) Descriptive statistics of the SVs count for each SV type.

(**b**) The count of SVs per sample by each SV type.

(**c**) SV count distribution by minor allele frequency (MAF) and size.

(**d**) Length distribution of SVs. The peaks represent the Alu, SVA, and LINE1 events.

(**e**) The count of SVs according to the predicted function region annotation by each SV type.

(**f**) The count of SVs per sample according to the predicted function region annotation by each SV type.

(**g**) Venn diagram showing the overlap between SVs in this study and published SV datasets. Among the SVs, 49.57% are novel, while 50.43% have been previously reported.

(**h**) The difference in SV counts between novel and reported SVs according to the predicted function region annotation.

(**i**) The counts of affected genes per genome by novel and reported SVs according to the predicted function region annotation. Differences between novel and reported SVs were assessed with

two-sided t-tests. CPXs were not included in this analysis due to a lack of accurate annotation of the genes they affected.

Abbreviations: SV, structural variant; DEL, deletions; DUP, duplications; INS, insertions; INV, inversions; CPX, complex variants; CNV, copy number variation.

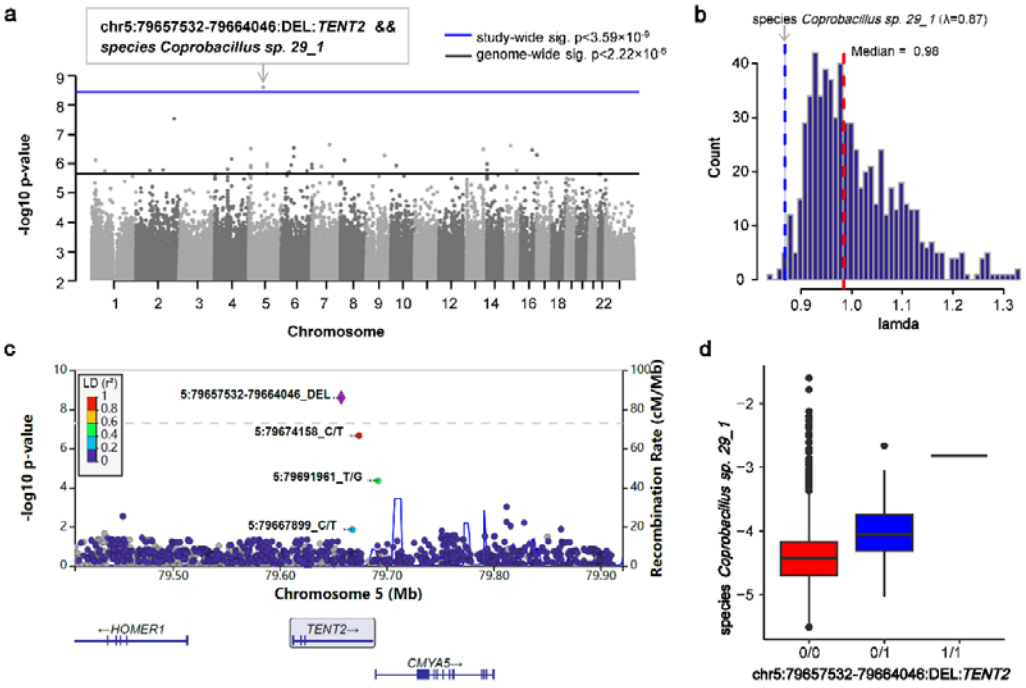


**Figure 2. Genome-wide associations of SVs with the gut microbiome identified by mbGWAS.**

(**a**) Manhattan plot representing the GWAS results (619 microbial features; 22,519 common high-quality SVs with MAF ≥ 1%). The y-axis indicates the log10-transformed p-values, while the x-axis indicates the genomic positions of the SVs. The study-wide significance ($p < 3.59 \times 10^{-9}$) and genome-wide significance ($p < 2.2 \times 10^{-6}$) are indicated by horizontal lines colored blue and black, respectively. The annotations highlight the study-wide association of deletion variant at the intronic region of *TENT2* gene and the species *Coprobacillus sp. 29_1*.

(**b**)The distribution of genomic inflation factor (λ) for 616 mbGWAS tests, ranging from 0.84 to 1.33 with a median value of 0.98. The λ of GWAS for species *Coprobacillus sp. 29_1* is 0.87.

(**c**) The regional plot showing mbGWAS results of the *TENT2* deletion (purple diamond) and its nearby SNPs associated with the species *Coprobacillus sp. 29_1*.

(**d**) The log-transformed relative abundances of *Coprobacillus sp. 29_1* in carriers of *TENT2* deletion and non-carriers.

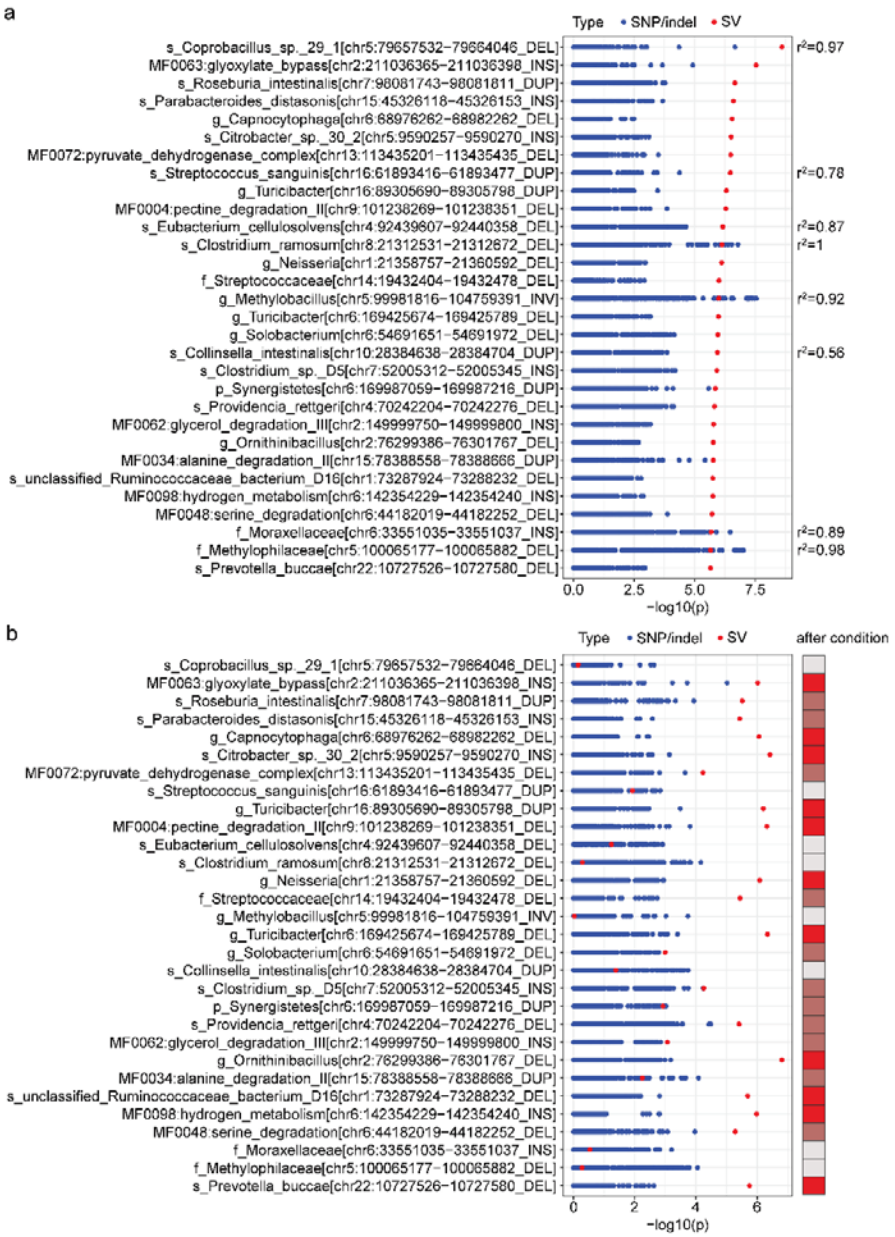


**Figure 3. The raw and conditional GWAS results for significant SVs and their nearby SNPs/indels with the gut microbiome.**

**(a)** The raw associations of SVs and their nearby SNPs/indels (flanking 500kb of the SV) with gut microbiome.

**(b)** The associations of SVs and their nearby SNPs after conditioning on the tagging SNP/indel showing the strongest LD with the SV. The bar in the right indicates the significance of SV association after conditional analysis, including no longer significant (colored in grey), not reaching genome-wide significant (colored in dark red) and retaining genome-wide significant (colored in red).

The x axis indicates the log10-transformed p values. The y axis indicates the associations of the SVs and nearby SNPs/indels with gut microbiome (N = 30). The red dots represent the p-values associated with SVs, and the blue dots represent the p-values associated with SNPs/indels.

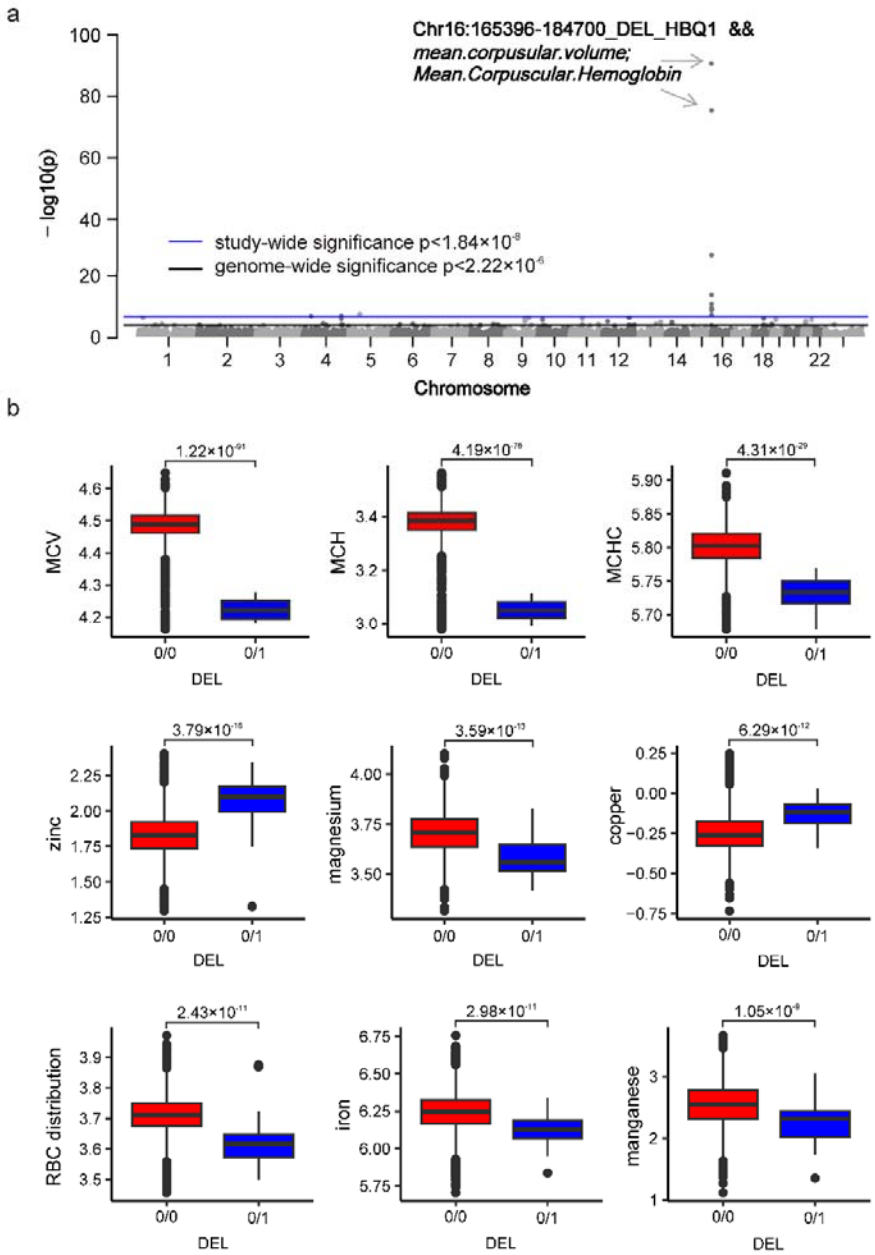


**Figure 4. Genome-wide associations of SVs with blood metabolites.**

(**a**) Manhattan plot depicting the GWAS results (121 blood metabolite traits; 22,519 common high-quality SVs with MAF ≥ 1%). The study-wide significance ($p < 1.84 \times 10^{-8}$) and genome-wide significance ($p < 2.2 \times 10^{-6}$) are indicated by horizontal lines colored blue and black, respectively. The annotations show the DEL variant on chromosome 16 (chr16: 165396-184700), corresponding to the *HBA1*, *HBA2*, *HBM*, and *HBQ1* genes.

(**b**)Boxplots of nine blood metabolite levels associated with the *HBA1/HBA2/HBM/HBQ1* DEL that passed study-wide significance, comparing the metabolite levels between DEL carriers ("0/1": individuals with DEL) and non-carriers ("0/0": individuals without DEL).

MCV, mean corpuscular volume; MCH, mean corpuscular hemoglobin; MCHC, mean corpuscular hemoglobin Concentration; RBC distribution, red blood cell distribution.

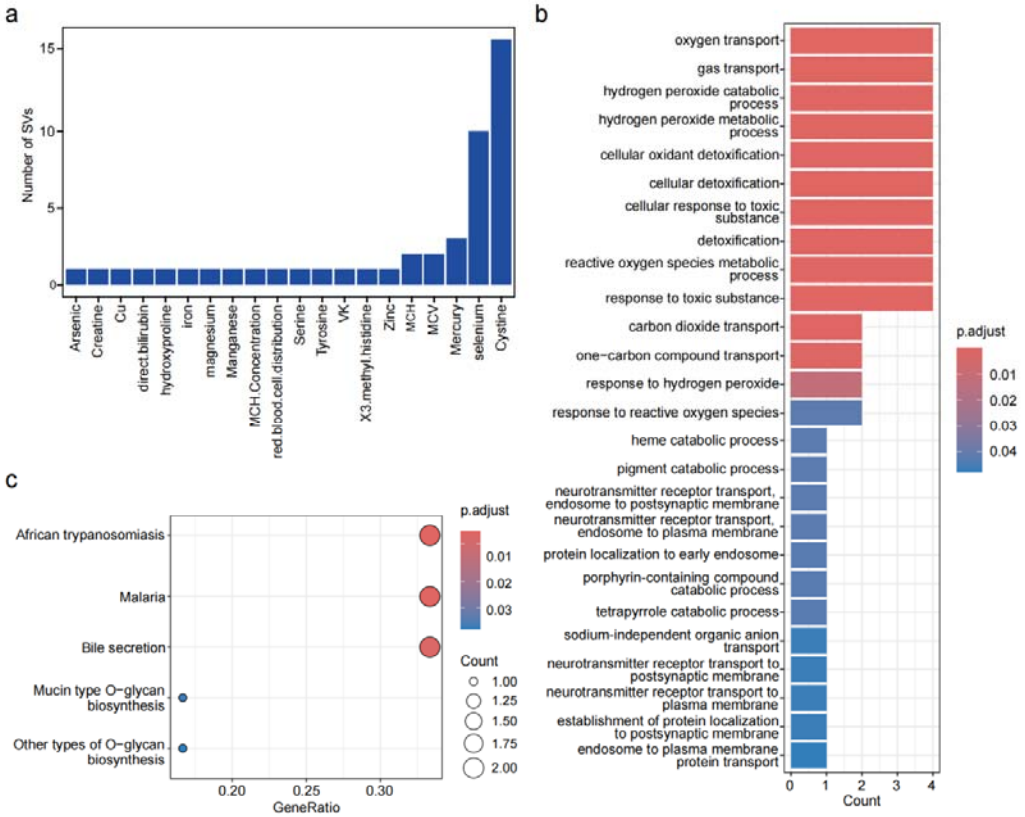


**Figure 5. The enrichment analysis of significantly associated SVs in blood metabolites.**

(**a**)The distribution shows the number of SVs significantly associated with blood metabolites (N=48).

(**b and c**) GO (b) and KEGG enrichment analysis (c) for genes harboring SVs significantly associated with the blood metabolites. The bar plot (b) only displays the biological process (BP) results from the GO analysis terms.

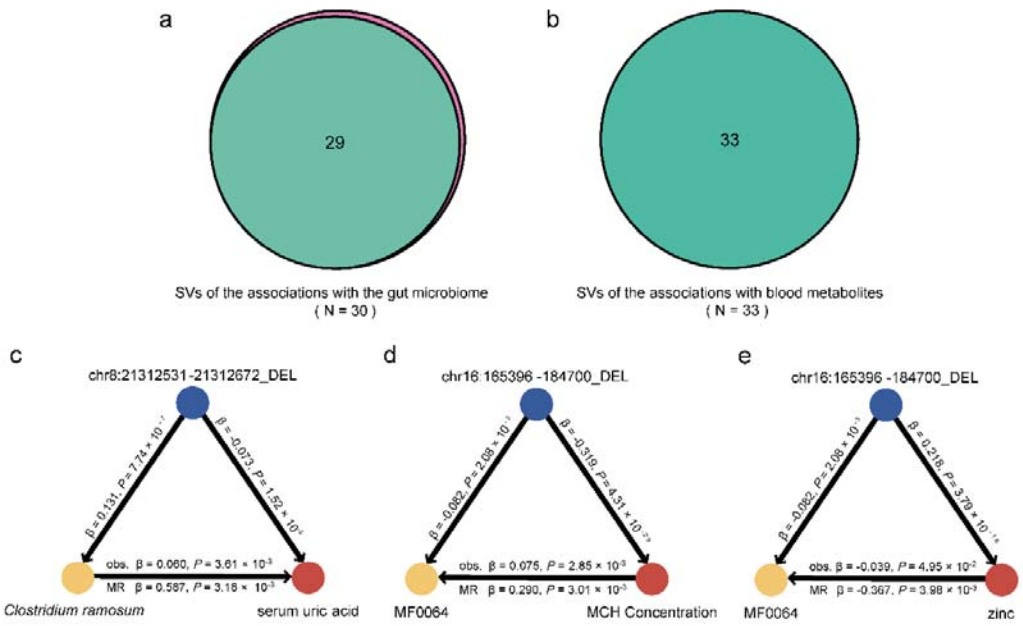


**Figure 6. Interactions between the gut microbiome and blood metabolites supported by SVs.**

(a) Venn diagrams showing the number of overlapped SVs significantly associated with the gut microbiome ($p < 2.2 \times 10^{-6}$) that also linked to blood metabolites ($p < 0.05$).

(b) Venn diagrams showing the number of overlapped SVs significantly associated with the blood metabolites ($p < 2.2 \times 10^{-6}$) that also linked to the gut microbiome ($p < 0.05$).

(c) The deletion on chromosome 8 (SV length: 141 bp) is significantly associated with both *Clostridium ramosum* ($\beta = 0.131$, $p = 7.47\times10^{-7}$) and the blood metabolite serum uric acid ($\beta = 0.073$, $p = 1.52\times10^{-3}$). A significant observational correlation and further causal effect of *Clostridium ramosum* on serum uric acid was supported by MR.

(d) The causal effect of MCHC on MF0064: the triacylglycerol degradation supported by their overlapped genetic SV, such as the HBA1/HBA2/HBM/HBQ1 deletion (chr16:165396-184700_DEL).

(e) The causal effect of zinc on MF0064: the triacylglycerol degradation supported by their overlapped genetic SV, such as the HBA1/HBA2/HBM/HBQ1 deletion (chr16:165396-184700_DEL).

Obs., observational correlation; MR, Mendelian randomization.